Targeting Orthosteric and Allosteric Pockets of Aromatase via Dual-Mode Novel Azole Inhibitors

09 March 2025

Targeting orthosteric and allosteric pockets of aromatase via dual-mode novel azole inhibitors

Jessica Caciolla,[§,a] Angelo Spinello,[§,b] Silvia Martini,[c] Alessandra Bisi,[a] Nadia Zaffaroni,[c] Silvia Gobbi,[a,*] and Alessandra Magistrato[b,*]

a) Department of Pharmacy and Biotechnology, Alma Mater Studiorum-University of Bologna, via Belmeloro 6, 40126, Bologna, Italy.

b) CNR-IOM Democritos c/o International School for Advanced Studies (SISSA), Via Bonomea 265, Trieste, Italy.

c) Fondazione IRCSS Istituto Nazionale dei Tumori, via Amadeo 42, 20113, Milano, Italy.

Abstract

Breast cancer (BC) is the most diffused cancer type in women and the second leading cause of death among female population. Effective strategies to fight estrogen responsive (ER+) BC, which represent the 70% of all BC cases, rely on estrogen deprivation, via the inhibition of the aromatase enzyme, or the modulation of its cognate estrogen receptor. Current clinical therapies significantly increased patient survival time. Nevertheless, the onset of resistance in metastatic BC patients undergoing prolonged treatment regimens is becoming a current clinical challenge, urgently demanding for devising innovative strategies. In this context, here we designed, synthesized and performed in vitro inhibitory tests on the aromatase enzyme and distinct ER+/ER- BC cell line types of novel azole bridged xanthones active in the low μM range, which behave as dual-mode inhibitors, being able to target both the orthosteric and the allosteric site of the enzyme placed along one access channel. Multiscale classical and quantum-classical molecular dynamics simulations of the new compounds, as compared with other steroidal and non-steroidal inhibitors, provide a rational to their observed inhibitory potency, and supply the guidelines to boost the activity of inhibitors able to exploit coordination to iron and occupation of the access channel to modulate estrogen production.

§ Authors equally contributed to the work

- Correspondence to alessandra.magistrato@sissa.it, silvia.gobbi@unibo.it

Breast cancer (BC) is the most common malignancy in women and ranks the second place among cancer-related death in female gender. Recently, the advances in genomics have clarified that BC is a heterogeneous disease, and different biological subtypes can be recognized, leading to therapeutic choices based also on tumor genetic profiling.[1,2] Considering that approximately 75% of patients are hormone receptor positive, meaning that estrogens are needed for tumor's progression, therapy focused on estrogen deprivation plays nowadays a pivotal role. Indeed, these patients can be treated, mainly after surgery, with hormonal therapy alone, bypassing the more toxic chemotherapy, with a relatively favorable prognosis. Targeted therapy of BC is now based on two different approaches. Interference with binding of estrogens to their receptors (ERα) can be obtained via selective estrogen receptor modulators (SERMs), such as the prototype tamoxifen[3] (Fig. 1), and selective estrogen receptor degraders (SERDs), such as fulvestrant[4] (Fig. 1). Tamoxifen, belonging to the SERM category of drugs, shows high binding affinity for ERs and is used to significantly reduce the chance of BC in high/average-risk women, even though it becomes ineffective in relapsing metastatic BC patients.[5] Alternatively, more recently marketed drugs act by affecting the synthesis of estrogens via inhibition of the cytochrome P450 (CYP450) aromatase, key enzyme for their biosynthetic process.[6] Human aromatase (HA), produced by the *CYP19A1* gene on the chromosome 15q21.2, catalyzes aromatization of androgens to estrogens, with a unique pathway in the steroidal hormone biosynthesis.[7-9] This enzyme is found in all estrogen producing tissues, such as ovaries and adrenal glands, but also in estrogen positive tumor cells. Its inhibition induces a cascade of events at molecular level, including both downregulation of a number of estrogens associated genes implicated in cell proliferation and up-regulation of genes associated with immunological response and cell adhesion. Third-generation steroidal and non-steroidal aromatase inhibitors (AIs, exemestane, letrozole and anastrozole, Fig. 1) are now considered as first-line treatment for hormone-dependent BC.[1,2]

In spite of the unquestionable effectiveness of current therapies, hurdles regarding compliance with the diverse side effects of SERMs and AIs and the development of resistance still need to be solved, keeping ERα and HA as very attractive targets.[2,10] Although a comprehensive picture of the molecular mechanisms involved in resistance onset is still missing, large-scale genomic investigations have identified aggressive ER somatic mutations, which make the receptor intrinsically active, even in the absence of estrogens.[5] As a result, the strategy of completely abrogating estrogen production loses its efficacy in these aggressive ER mutant isoforms.

Remarkably, a milestone in the rational design of AIs was the release of HA crystal structure,[11] which fostered intense investigations on the functional aspect of this CYP450[12-14] and boosted the search for novel AIs.[15-17]
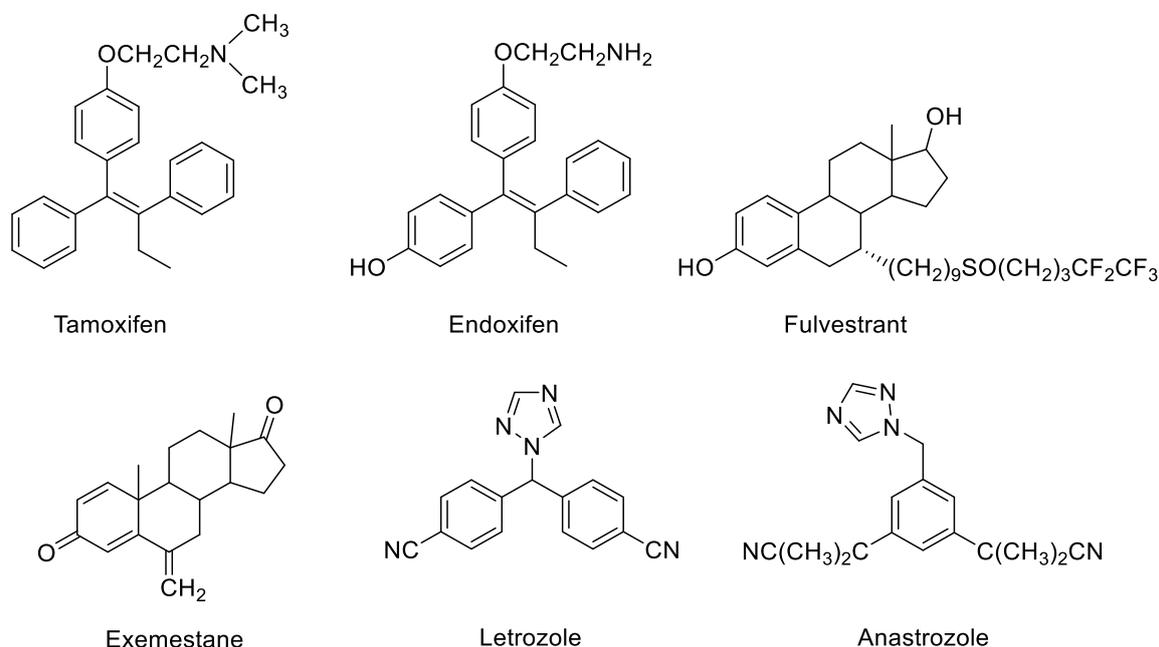
Figure 1. Molecular structures of selective estrogen receptor modulators (SERMs, Tamoxifen and its metabolite Endoxifen) and degraders (Fulvestrant), along with the third-generation aromatase inhibitors (AIs, Exemestane, Letrozole and Anastrozole).

Nevertheless, the need of catching alternative strategies to counteract resistance onset to current therapies led to the exploitation of alternative inhibitory/modulatory estrogen production mode. In this context, allostery was praised as a possible viable route to fine-tune estrogen production. Indeed, some primary metabolites of tamoxifen, still endowed with significant ER modulation properties, were found to act as AIs as well,[18] and this was supposed to contribute to the overall pharmacological effect of the drug. In particular, kinetic studies showed for endoxifen (Fig. 1) a non-competitive inhibition mechanism,[18] suggesting its potential interaction with different binding sites in the enzyme. Non-competitive or mixed inhibition mechanism was also claimed for the marketed AI letrozole (LTZ), for other azole compounds used as pesticides.[19] In a previous study, we identified allosteric binding pockets potentially responsible for this non-active site-directed inhibition.[20] Among these sites, one pocket overlapped with the heme proximal cavity, and a ligand binding at this site may prevent the coupling of HA with NADPH-cytochrome P450 reductase (CPR), and, thus, the electron flow necessary for catalysis; the second pocket was placed along one possible access/egress channel of the substrate/product to/from the active site, and the interaction of a ligand with this site may result in blocking the substrate entrance to the active site. These sites were recently targeted by

distinct inhibitor types to fine-tune HA activity for therapeutic benefit.[21] Moreover, aiming at the development of steroidal inhibitors' derivatives via the functionalization of exemestane (EXE), it was noted that the addition of a hydrophobic tail tailored to occupy the allosteric cavity lying along one of the HA's access channels resulted in nM inhibition, suggesting that the simultaneous occupation of the orthosteric and allosteric sites may be an effective inhibition strategy.[22,23]

As part of a long-lasting project aimed at developing novel non-steroidal structures endowed with HA inhibiting activity, some of us developed a series of imidazolylmethylxanthones (Fig. 2), which resulted to be potent and selective AIs.[24] The position of the chain carrying the heme-coordinating imidazole moiety on the central core was varied and proved to remarkably affect the potency of the compounds, ranging from μM to nM (potency ranking: position 4>1>3>2, Table 1).

imidazolylmethylxanthones   alkynyloxy derivatives
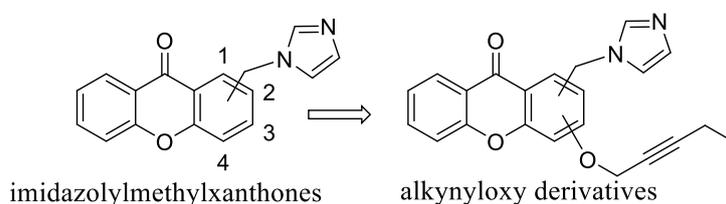
Figure 2. Design of potential dual-binding xanthone derivatives.

In this paper, we exploit this dual-mode inhibition strategy by designing *in silico* new derivatives of previously reported xanthones (Fig. 2) via the insertion of a pentynyloxy chain, which literature reported as the most suitable functional group for a favorable interaction with the hydrophobic residues lining the access channel when inserted on steroidal AIs.[22] To identify novel competitive HA inhibitors, docking calculations were initially performed following a protocol successfully used in previous studies.[15] The calibration of the protocol and its accuracy were assessed by docking the most active imidazolylmethylxanthones compounds previously reported (**1**-**3**, Fig. 3a).[24]
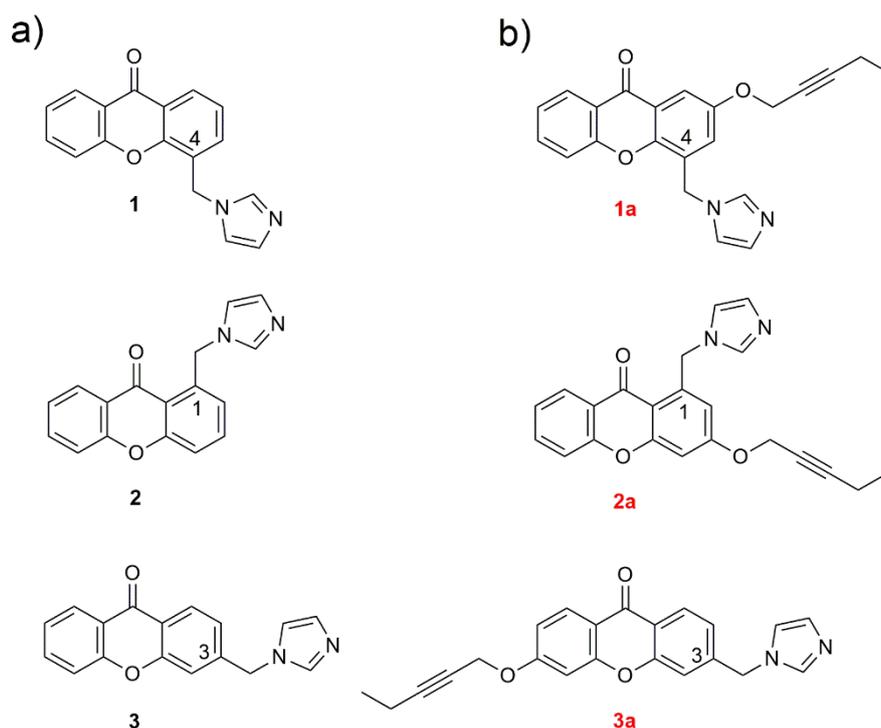
Figure 3. a) Previously reported imidazolylmethylxanthones[24] and b) the newly synthesized compounds designed on the basis of docking simulations.

Surprisingly, a standard docking protocol failed in finding binding poses in which the imidazole nitrogen was able to coordinate the heme moiety, consistently with previous findings.[25-27] Since the high potency of clinically employed non-steroidal AIs (e.g. letrozole, anastrazole) is commonly attributed to the formation of a coordination bond between the nitrogen of the azole ring and the heme iron atom, and, since docking programs do not account for the formation of covalent/coordination bonds, especially with transition metal ions,[28] here docking calculations were done by imposing a constraint between the Fe@heme -N@azole atoms. This approach generated binding poses with the imidazole ring in the proximity of the heme iron atom (Fig. 4). In particular, the azole nitrogen of compound **1** laid at a distance of 2.47 Å from the iron and the imidazole ring adopted a suitable binding geometry (i.e. almost perpendicular to the heme plane). Furthermore, the aromatic moiety of the xanthone established π-stacking interactions with Trp224. As well, **2** nicely fitted in the binding pocket, although exhibiting a longer Fe-N distance (3 Å). The best binding pose of compound **3**, which possessed the highest IC_{50} among the previously reported imidazolylmethylxanthones series, showed a considerable tilt of the azole ring with respect to the heme plane, possibly resulting in a lack of coordination. Nevertheless, the xanthone also established π-stacking interactions with Phe134. Thus, the observed binding poses provide a coarse rationale for the experimentally observed trend of IC_{50}s (Fig. 3a). To further assess the reliability of our docking protocol, we predicted the binding pose of letrozole (LTZ), belonging to the third-generation AIs (Fig. 1). Stunningly, even when introducing

6

in the docking protocol a constraint to the Fe-N distance, we did not obtain a binding pose. This is consistent with the absence of any crystallographic structure for this inhibitor in complex with HA, suggesting that a considerable deformation of the active site is required for this drug to fit into the catalytic pocket. Hence, we adopted an induced fit protocol,[29] in which the side chains of the binding site can be displaced to accommodate the ligand, resulting in a binding pose with a Fe-N distance of 2.40 Å and in which one cyano group of LTZ was hydrogen (H)-bonding to the backbone of Met374 (Fig. 4). The second cyano group, instead, laid at the entrance of the access channel.

Taking advantage of the recent successful functionalization of steroidal inhibitors,[22,23] and based on the docking poses of compounds **1**-**3** (Fig. 4) we designed new derivatives (Fig. 3b) by functionalizing the imidazolylmethylxanthones with a pentynyloxy chain. In order to fill the entrance of the access channel (Fig. 4), functionalization in the ortho or meta positions with respect to the imidazole ring appeared as the most suitable. Nevertheless, docking calculations, imposing a constraint on the Fe-N bond, identified binding poses only for compounds **1a** and **2a** bearing the hydrophobic tail in the meta position (Fig.s 3b and 4). These exhibited a Fe-N distance of 2.82 and 2.52 A, respectively, with the pentynyloxy chain located within the access site, similarly to C6-substituted steroidal inhibitors.[22] Moreover, compound **2a** established π-stacking interaction with Trp224.

Considering the binding pose of compound **3**, the entrance of the access channel could not be easily reached by the introduction of the rigid alkyloxy chain. Yet, from preliminary docking calculations without the Fe-N metal constraint, the resulting binding pose displayed the carboxy oxygen of the aromatic moiety located in proximity of the iron atom. Thus, exploiting this possible interaction mode, we designed a ligand (**3a**) in which the alkyloxy chain and the imidazolylmethyl moiety are located at symmetric positions on different rings of the xanthone. In this case, a constrained induced fit protocol led to a binding pose in which the oxygen of the xanthone was at 2.57 Å from the iron atom, while the pentynyloxy chain was located in a hydrophobic pocket lined by residues Leu301, Leu305, Leu25, Tyr220, Ile125 and Met127 (Fig. 4).
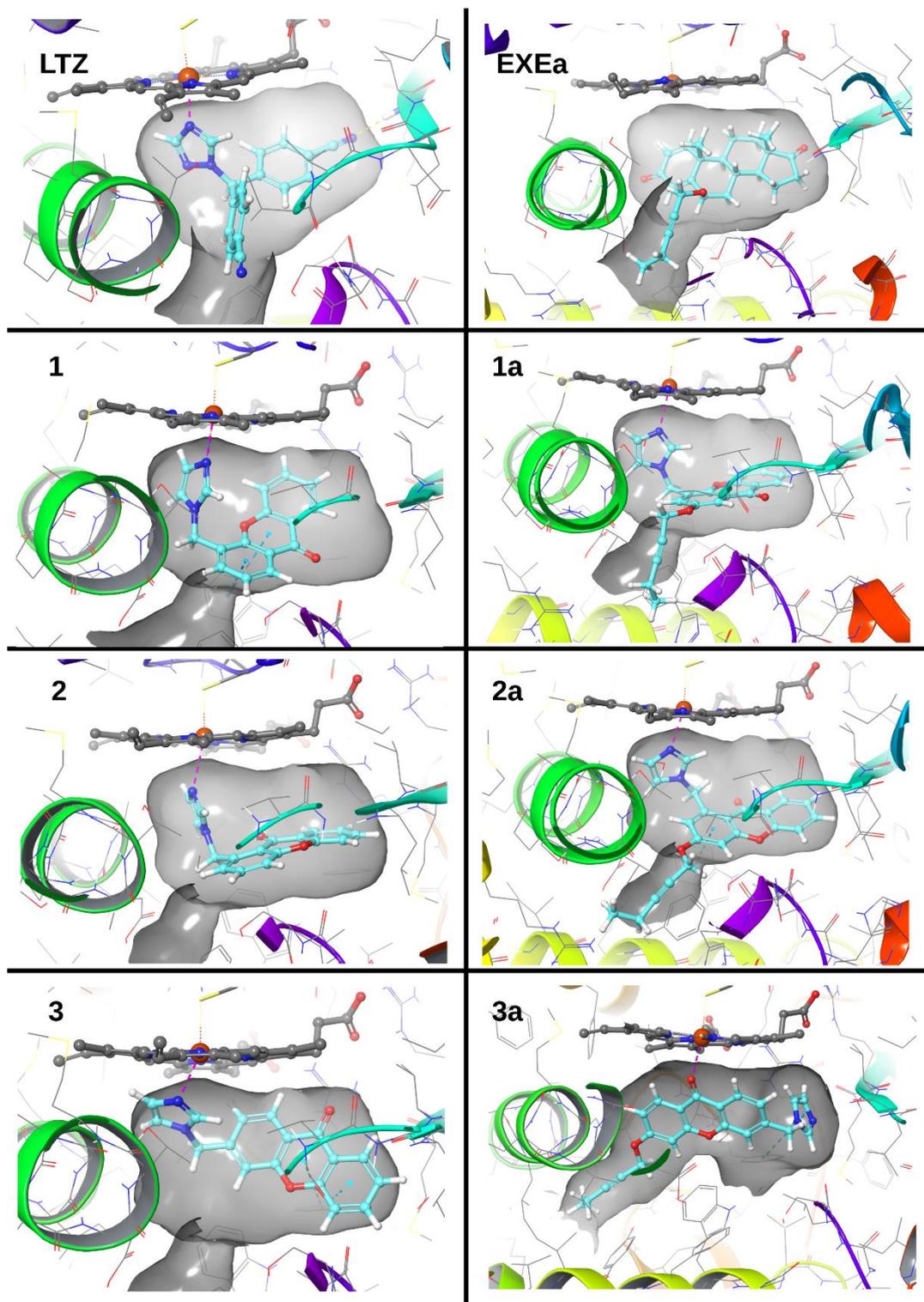
Figure 4. Best-ranked binding poses obtained for the AIs letrozole, exemestane functionalized with a pentynyloxy chain (EXEa)[22] and for compounds **1**-**3**, **1a**-**3a**. The protein is shown in ribbons, the binding site is highlighted with a transparent gray surface, while the inhibitors and the heme are shown in a ball and stick representation.

For the synthesis of the designed alkynyloxy-substituted xanthones **1a** and **2a** (Scheme 1), 4-methoxy-2-methylphenol, obtained from the reduction of 2-hydroxy-5-methoxybenzaldehyde,[30] or the commercially available 3-methoxy-5-methylphenol were reacted with 2-chlorobenzoic acid under Ullmann reaction conditions to give the corresponding diarylethers, which were then cyclized by treatment with polyphosphoric acid to obtain the xanthone cores (**4**, **7**). Bromination of the methyl group with NBS and subsequent reaction with imidazole allowed obtaining the intermediates **5** and **8**, which were then demethylated with $AlCl_3$ to give the corresponding hydroxyl derivatives **6** and **9**, and successively alkylated with 1-bromo-2-pentyne to get the final compounds.

Scheme 1
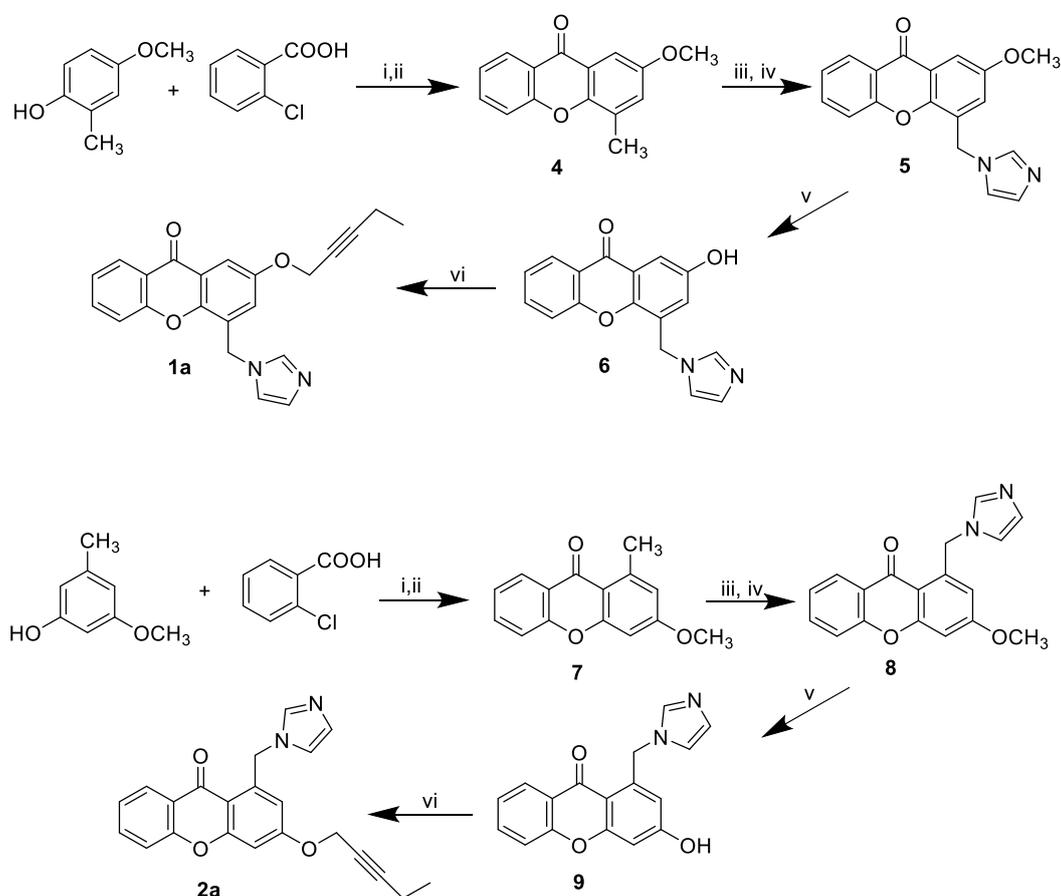
Reagents and conditions: i) K_2CO_3, Cu/CuI, pyridine, H_2O, reflux, 2 h; ii) H_3PO_4, P_2O_5, 120 °C, 7 h; iii) NBS, BPO, CCl_4, reflux, hv, 6 h; iv) imidazole, CH_3CN, reflux, N_2, 6 h; v) $AlCl_3$, toluene, reflux, 3 h; vi) 1-bromo-2-pentyne, K_2CO_3, acetone, reflux, 18-26 h.

For the synthesis of xanthone **3a**, 6-methoxy-3-imidazolylmethylxanthone **10**[31] was subjected to the demethylation step followed by alkylation with 1-bromo-2-pentyne, as reported for xanthones **5** and **8**, to obtain the desired compound (Scheme 2).

Scheme 2
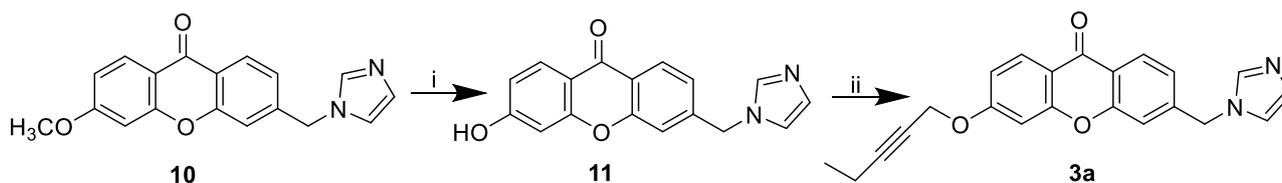
Reagents and conditions: i) AlCl$_3$, toluene, reflux, 3 h; ii) 1-bromo-2-pentyne, K$_2$CO$_3$, acetone, reflux, 18-26 h.

The inhibitory potency against HA of the newly synthesized compounds (**1a-3a**) was then tested at different concentrations (from 0.1 to 100 μM) to obtain IC$_{50}$ values, which proved to be in the low μM range (from 0.77 to 5.55 μM). Thus, for derivatives **1a** and **2a** a marked reduction of the inhibitory potency as compared to their parent compounds was observed,[24] whereas **3a** retained a similar activity with respect to **3** (Table 1). It seemed, thus, clear that the introduction of a long and rigid alkoxy chain close to the imidazole moiety (as in **1a** and **2a**) resulted in an impairment for the appropriate positioning of the compounds in the active site of the enzyme, while the same chain located at the opposite side on the scaffold (**3a**) did not quite influence the interaction with the target. Moreover, the ability of compounds **1-3** and **1a-3a** to inhibit the growth of ER+ (MCF-7) and ER- (MDA-MB-231) cell lines, expressed by the Growth Inhibition activity (GI$_{50}$) values, was also evaluated (Fig.s S1 and S2). No appreciable differences were observed in the sensitivity of the analyzed cell lines, and this could possibly be related to the previously reported comparable expression of aromatase in MCF-7 and MDA-MB-231 cells[32] and the specificity of the compounds towards the target. Among the six tested compounds, the previously reported **1-3** showed modest antiproliferative activities, with GI$_{50}$ values > 10 μM. As regards the new substituted compounds, the same range of potency was seen with compound **1a**, while **2a** displayed a GI$_{50}$ < 10 μM in MCF-7 (although not in MDA-MB-231) cell lines, comparable to LTZ.[21] This observation suggests that the introduction of the alkoxy chain led to an increase in antiproliferative activity for compounds **1a** (only on MDA-MB-231 cells) and particularly for **2a** (on both cell lines) with respect to parent compounds **1** and **2**. On the contrary, **3a** was not able to inhibit cell growth at any concentration considered in both cell models, and the peculiar behavior of this compound may be ascribed to the different positioning of the long and rigid alkoxy chain as compared to **1a** and **2a**, for which the chain is placed on the same phenyl ring of the imidazolyl substituent.

Table 1. IC$_{50}$s obtained on the isolated enzyme and GI$_{50}$s on ER+ (MCF-7) and ER- (MDA-MB-231) cell lines, distances between the nitrogen atom of the ligands and the iron atom of the heme and the angle between the planes of the imidazole ring and the heme moieties are reported from left to right columns, respectively.

Compound	IC$_{50}$ (µM)	GI$_{50}$ MCF-7 (µM)	GI$_{50}$ MDA-MB-231 (µM)	Distance (Å)	Angle (°)
LTZ	0.01 [19]	4.1 ± 1.1 [21]	> 10 [21]	2.33 ± 0.15	91.8 ± 2.7
1	0.017 [24]	69.1 ± 0.8	58.3 ± 11.7	2.30 ± 0.13	88.8 ± 2.0
2	0.150 [24]	59.0 ± 2.6	44.3 ± 6.5	2.31 ± 0.15	89.0 ± 2.6
3	0.390 [24]	19.9 ± 5.9	30.4 ± 4.6	2.23 ± 0.12	91.3 ± 2.1
1a	5.55 ± 2.3	52.3 ± 16.3	21.1 ± 9.3	2.18 ± 0.10	92.3 ± 2.2
2a	2.85 ± 0.1	6.3 ± 1.1	17.5 ± 7.9	2.15 ± 0.08	91.8 ± 2.4
3a	0.77 ± 0.3	> 100	> 100	---	---

[a] Concentration of drug required to inhibit cell growth by 50% as determined after 72 hrs continuous exposure to the tested compounds. Data represent the mean ± standard deviation of three independent experiments.

In order to dissect the molecular facets underlying the observed inhibitory potency of the dual-mode compounds synthesized here, we applied a sophisticated computational workflow, able to accurately describe the formation of the coordination bond between imidazole rings of the inhibitors and the iron atom of the heme moiety: i) first, classical molecular dynamics (MD) simulations constraining the Fe–N bond distance were performed to relax the protein, and, next, ii) quantum mechanics/molecular mechanics (QM/MM) MD simulations were done to account for the coordination bond and the binding of the inhibitors to the enzyme.[33] Due to the high computational costs of this latter type of calculations, if the formation of the Fe-N coordination bond was not occurring within 5 ps of QM/MM MD simulation, we performed metadynamics (MTD) simulations, using as collective variable (CV) the Fe-N distance to induce the formation of the coordination bond (See Methods section). The binding pose obtained in this manner was the further relaxed by unbiased 10 ps long QM/MM MD. For all investigated compounds, we observed the formation of stable coordination bonds between the imidazole rings and the heme moiety (Fig. 5) with the exception of compound **3a**. Indeed, for the latter the potential coordination bond, observed in the docking pose, was lost during the QM/MM MD simulation. We, next, accurately monitored the structural parameters obtained from QM/MM MD and we compared them with the clinically used LTZ drug, in order to identify structural traits that may provide a rationale to the observed experimental data (Table 1). Despite the different potency, all compounds exhibit similar Fe-N bond lengths, with **1a** and **2a** being slightly shorter (2.18 and 2.15 Å, respectively). As well, a similar trend could be observed for the average angle between the planes composed by the imidazole ring of the inhibitors and the heme, which were almost perfectly perpendicular. These evidences suggest that the coordination bonds length and orientation of the azole group is not critical for the reported IC$_{50}$s.
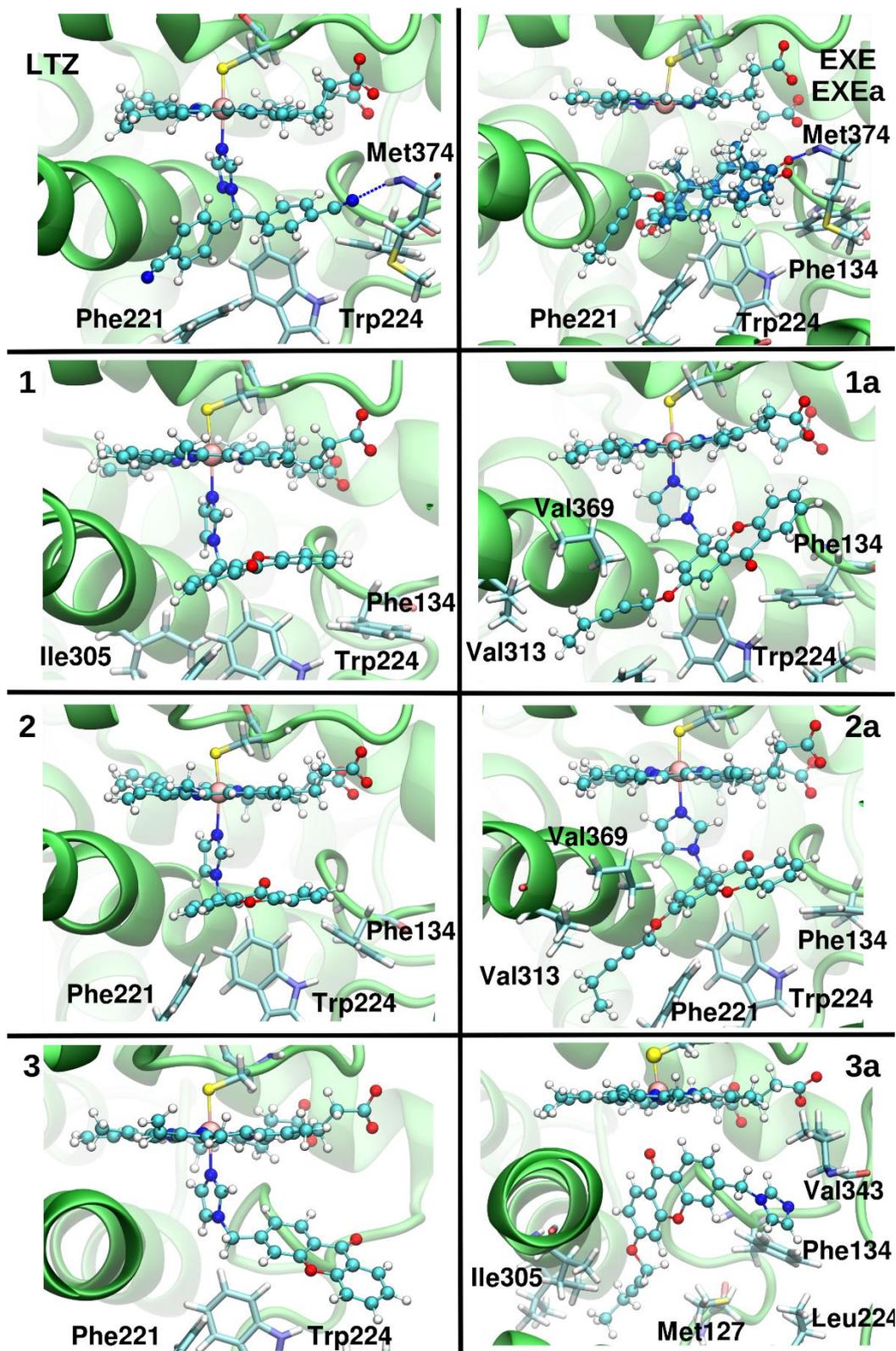
Figure 5. Representative structures as obtained from quantum-classical molecular dynamics simulations of letrozole (LTZ), exemestane (EXE) and its derivative (EXEa),[22] compounds **1-3** and **1a-3a**. For comparison, the dual mode steroidal inhibitor EXEa is also reported superimposed to EXE. The inhibitors and the heme moiety are shown in a ball and stick representation, while hydrophobic residues involved in stacking and hydrophobic interactions are highlighted as sticks. When present, hydrogen bonds are shown as dashed red and blue lines.

Table 2: The energetic costs of the active site rearrangements upon binding of the distinct drugs are considered as the protein internal energies obtained with the Molecular Generalized Born Surface Area (MM-GBSA) method and are reported as the sum of the internal bonds, angles and dihedrals protein contributions.

	Bond	**Angles**	**Dihedrals**	**Total**
LTZ	1740.3 ± 89.2	3166.5 ± 104.2	6802.4 ± 40.7	**11709.2** ± 143.1
EXE	54.0 ± 8.4	3864.8 ± 43.3	5835.2 ± 27.3	**9754.0** ± 51.9
EXEa	48.2 ± 0.8	3861.6 ± 43.3	5828.6 ± 29.6	**9738.4** ± 52.5
1	2083.1 ± 47.2	3519.2 ± 50.7	6791.7 ± 36.9	**12394.0** ± 78.5
1a	2089.6 ± 39.6	3523.6 ± 35.6	6879.0 ± 37.9	**12492.2** ± 65.4
2	1933.0 ± 30.2	3314.8 ± 52.8	6810.3 ± 40.9	**12058.1** ± 73.3
2a	1862.6 ± 32.3	3306.9 ± 41.8	6785.1 ± 34.3	**11954.6** ± 63.0
3	1901.7 ± 33.1	3351.7 ± 46.3	6798.9 ± 31.6	**12052.3** ± 65.1
3a	1961.3 ± 31.7	3374.9 ± 41.2	6829.4 ± 26.3	**12165.6** ± 58.3

Surprisingly, the Fe-N distances calculated for **1a** and **2a** are similar to that of LTZ, suggesting that a perfect coordination geometry of the ligand to the heme iron atom is not the key element underlying its inhibitory activity. Nevertheless, LTZ, besides coordinating the heme iron, engages a persistent H-bond with Met374 and hydrophobic interactions with several residues located in the catalytic pocket (Phe221, Trp224, Phe132, Leu477, Val370, Leu372 and Ile133). These may be both critical elements to boost the LTZ potency. The steroidal inhibitor EXE lays in the active site showing a binding pose that perfectly resembles that of the endogenous substrate androstenedione. EXE H-bonds with Asp309[34] and the backbone of Met374, similarly to LTZ (Fig. 5). In this case, the addition of the hydrophobic tail does not alter the binding mode in the cavity and this protrusion snugly fits in the allosteric site (Fig. 5).[22] As a further element to explain the trend of potency, we also monitored the energetic costs of the active site rearrangements upon binding of the distinct drugs by considering the protein internal energies (Table 2). While EXE and its pentynyloxy-substituted derivative EXEa possess a similar deformation energy, compounds **1** and **3** show lower deformation values when compared to their derivatives **1a** and **3a**, suggesting that the presence of the tail imposes a strain in the orthosteric and allosteric sites.

Finally, to exclude that the increased size of the ligands may have hampered their binding to the active site, and that their inhibitory activity may be ascribed to a non-active site-directed inhibition, we performed docking calculations, followed by classical MD simulations on the two allosteric pockets successfully exploited in our previous study.[21] Only compound **3a** was able to fit inside HA access channel (Site 1, Fig. S3), however, it suddenly dissociated after few nanoseconds in classical MD simulation. In the case of the heme proximal cavity (Site 2), the putative binding site of HA redox partner (CYP450 reductase), compounds **1a**-**3a** spontaneously dissociated after 50 ns of MD simulations (Fig. S4).

Over the last four decades, aromatase enzyme has been a key target for the treatment and, more recently, prevention of ER+ BC. In this respect, although the release of the first HA crystal structure was a milestone for designing novel inhibitors, conventional docking methods experienced challenges to accurately describe the correct binding pose of AIs which form coordination bonds with the iron atom of the heme.[2] This has heavily plagued research efforts in the rational design of a novel generation of AIs. Moreover, this prompted the need of a higher level of theory to properly describe the coordination geometry, which however comes at high computational cost, long simulation time and can be applied to a limited number of molecules.[28,35]

Along this line, we have here exploited a complex computational protocol based on docking, classical and QM/MM biased and unbiased MD simulations to design and identify suitable binding poses of imidazolylmethylxanthones ligands' derivatives able to inhibit HA targeting both the orthosteric and allosteric sites. In spite of the *in silico* prediction, the designed and synthesized compounds did not undergo a boost of potency, as revealed by in vitro enzymatic assays, being able to inhibit the enzyme in the low μM range. In contrast, the GI_{50} of **2a** improved in cell-based studies.

A detailed structural analysis revealed that the addition of a pentynyloxy chain to imidazolylmethylxanthones, resulting in compound **1a** and **2a**, does not markedly affect the coordination geometry of the azole moiety to the iron atom and the pentynyloxy chain fits within the access channel, suggesting that the design of dual-mode non-steroidal inhibitors is very subtle. The fact that the coordination to heme iron is not pivotal to boost potency is also confirmed by compound **3a**, which has an IC_{50} similar to compound **1a** and **2a** even though it is not coordinating the iron atom. By analyzing in detail the differences observed with more active compounds we note that compounds **1a** and **2a** are unable to establish H-bonds interaction with the active site, at variance of the third-generation AIs LTZ and EXE, and do not exploit at best the hydrophobic and π-stacking interactions. Moreover, an energetic analysis clearly discloses that the pentynyloxy-substituted ligands **1a** and **3a** impose steric strain in the orthosteric and allosteric sites (Table 2). These data unequivocally unveil that the design of small-molecule HA inhibitors with potency in the nM-low μM range depends on many different facts, among which the possibility of forming H-bonds and the deformation induced to the active site appear as the most relevant.

Besides rationalizing the critical structural elements underlying the activity of prototypical steroidal ad non-steroidal inhibitors, our outcomes provide critical guidelines for future development of next generation dual-mode inhibitors able to exploit allosteric and orthosteric sites of HA and possibly of other CYP450s, involved in cancer progression, to modulate steroid metabolism.

Supporting information

Experimental procedures for the syntheses, in vitro evaluation of compounds activities and simulation protocol and analysis; Figures S1 to S4. This material is available free of charge via the Internet at http://pubs.acs.org.

References

1.   Feng, Y.; Spezia, M.; Huang, S.; Yuan, C.; Zeng, Z.; Zhang, L.; Ji, X.; Liu, W.; Huang, B.; Luo, W.; Liu, B.; Lei, Y.; Du, S.; Vuppalapati, A.; Luu, H. H.; Haydon, R. C.; He, T. C.; Ren, G. Breast cancer development and progression: Risk factors, cancer stem cells, signaling pathways, genomics, and molecular pathogenesis. *Genes Dis.* **2018,** 5, 77-106.

2.   Spinello, A.; Ritacco, I.; Magistrato, A. Recent advances in computational design of potent aromatase inhibitors: open-eye on endocrine-resistant breast cancers. *Expert Opin. Drug Discov.* **2019,** 14, 1065-1076.

3.   Lewis, J. S.; Jordan, V. C. Selective estrogen receptor modulators (SERMs): mechanisms of anticarcinogenesis and drug resistance. *Mutat. Res.* **2005,** 591, 247-63.

4.   McDonnell, D. P.; Wardell, S. E.; Norris, J. D. Oral Selective Estrogen Receptor Downregulators (SERDs), a Breakthrough Endocrine Therapy for Breast Cancer. *J. Med. Chem.* **2015,** 58, 4883-7.

5.   Pavlin, M.; Spinello, A.; Pennati, M.; Zaffaroni, N.; Gobbi, S.; Bisi, A.; Colombo, G.; Magistrato, A. A Computational Assay of Estrogen Receptor alpha Antagonists Reveals the Key Common Structural Traits of Drugs Effectively Fighting Refractory Breast Cancers. *Sci. Rep.* **2018,** 8, 649.

6.   Ghosh, D.; Lo, J.; Egbuta, C. Recent Progress in the Discovery of Next Generation Inhibitors of Aromatase from the Structure-Function Perspective. *J. Med. Chem.* **2016,** 59, 5131-48.

7.   Simpson, E. R.; Mahendroo, M. S.; Means, G. D.; Kilgore, M. W.; Hinshelwood, M. M.; Graham-Lorence, S.; Amarneh, B.; Ito, Y.; Fisher, C. R.; Michael, M. D.; et al. Aromatase cytochrome P450, the enzyme responsible for estrogen biosynthesis. *Endocr. Rev.* **1994,** 15, 342-55.

8.   Spinello, A.; Ritacco, I.; Magistrato, A. The Catalytic Mechanism of Steroidogenic Cytochromes P450 from All-Atom Simulations: Entwinement with Membrane Environment, Redox Partners, and Post-Transcriptional Regulation. *Catalysts* **2019,** 9, 81.

9.   Spinello, A.; Pavlin, M.; Casalino, L.; Magistrato, A. A Dehydrogenase Dual Hydrogen Abstraction Mechanism Promotes Estrogen Biosynthesis: Can We Expand the Functional Annotation of the Aromatase Enzyme? *Chem. Eur. J.* **2018,** 24, 10840-10849.

10.   Augusto, T. V.; Correia-da-Silva, G.; Rodrigues, C. M. P.; Teixeira, N.; Amaral, C. Acquired resistance to aromatase inhibitors: where we stand! *Endocr. Relat. Cancer* **2018,** 25, R283-R301.

11.   Ghosh, D.; Griswold, J.; Erman, M.; Pangborn, W. Structural basis for androgen specificity and oestrogen synthesis in human aromatase. *Nature* **2009,** 457, 219-23.

12.   Sgrignani, J.; Magistrato, A. Influence of the membrane lipophilic environment on the structure and on the substrate access/egress routes of the human aromatase enzyme. A computational study. *J. Chem. Inf. Model.* **2012,** 52, 1595-606.

13.   Sgrignani, J.; Iannuzzi, M.; Magistrato, A. Role of Water in the Puzzling Mechanism of the Final Aromatization Step Promoted by the Human Aromatase Enzyme. Insights from QM/MM MD Simulations. *J. Chem. Inf. Model.* **2015,** 55, 2218-2226.

14.   Park, J.; Czapla, L.; Amaro, R. E. Molecular simulations of aromatase reveal new insights into the mechanism of ligand binding. *J. Chem. Inf. Model.* **2013,** 53, 2047-56.

15.   Caporuscio, F.; Rastelli, G.; Imbriano, C.; Del Rio, A. Structure-based design of potent aromatase inhibitors by high-throughput docking. *J. Med. Chem.* **2011,** 54, 4006-17.

16.   Favia, A. D.; Nicolotti, O.; Stefanachi, A.; Leonetti, F.; Carotti, A. Computational methods for the design of potent aromatase inhibitors. *Expert Opin. Drug Discov.* **2013,** 8, 395-409.

17.   Sgrignani, J.; Cavalli, A.; Colombo, G.; Magistrato, A. Enzymatic and Inhibition Mechanism of Human Aromatase (CYP19A1) Enzyme. A Computational Perspective from QM/MM and Classical Molecular Dynamics Simulations. *Mini Rev. Med. Chem.* **2016,** 16, 1112-24.

18.   Lu, W. J.; Desta, Z.; Flockhart, D. A. Tamoxifen metabolites as active inhibitors of aromatase in the treatment of breast cancer. *Breast Cancer Res. Treat.* **2012,** 131, 473-81.

19.   Egbuta, C.; Lo, J.; Ghosh, D. Mechanism of inhibition of estrogen biosynthesis by azole fungicides. *Endocrinology* **2014,** 155, 4622-8.

20.   Sgrignani, J.; Bon, M.; Colombo, G.; Magistrato, A. Computational approaches elucidate the allosteric mechanism of human aromatase inhibition: a novel possible route to Small-molecule regulation of CYP450s activities? *J. Chem. Inf. Model.* **2014,** 54, 2856-68.

21.   Spinello, A.; Martini, S.; Berti, F.; Pennati, M.; Pavlin, M.; Sgrignani, J.; Grazioso, G.; Colombo, G.; Zaffaroni, N.; Magistrato, A. Rational design of allosteric modulators of the aromatase enzyme: An unprecedented therapeutic strategy to fight breast cancer. *Eur. J. Med. Chem.* **2019,** 168, 253-262.

22.   Ghosh, D.; Lo, J.; Morton, D.; Valette, D.; Xi, J.; Griswold, J.; Hubbell, S.; Egbuta, C.; Jiang, W.; An, J.; Davies, H. M. Novel aromatase inhibitors by structure-guided design. *J. Med. Chem.* **2012,** 55, 8464-76.

23.   Roleira, F. M. F.; Varela, C.; Amaral, C.; Costa, S. C.; Correia-da-Silva, G.; Moraca, F.; Costa, G.; Alcaro, S.; Teixeira, N. A. A.; Tavares da Silva, E. J. C-6alpha- vs C-7alpha-Substituted Steroidal Aromatase Inhibitors: Which Is Better? Synthesis, Biochemical Evaluation, Docking Studies, and Structure-Activity Relationships. *J. Med. Chem.* **2019,** 62, 3636-3657.

24.   Gobbi, S.; Zimmer, C.; Belluti, F.; Rampa, A.; Hartmann, R. W.; Recanatini, M.; Bisi, A. Novel highly potent and selective nonsteroidal aromatase inhibitors: synthesis, biological evaluation and structure-activity relationships investigation. *J. Med. Chem.* **2010,** 53, 5347-51.

25.   Verras, A.; Kuntz, I. D.; Ortiz de Montellano, P. R. Computer-assisted design of selective imidazole inhibitors for cytochrome p450 enzymes. *J. Med. Chem.* **2004,** 47, 3572-9.

26.   Woo, L. W.; Bubert, C.; Sutcliffe, O. B.; Smith, A.; Chander, S. K.; Mahon, M. F.; Purohit, A.; Reed, M. J.; Potter, B. V. Dual aromatase-steroid sulfatase inhibitors. *J. Med. Chem.* **2007,** 50, 3540-60.

27.   Sgrignani, J.; Casalino, L.; Doro, F.; Spinello, A.; Magistrato, A. Can multiscale simulations unravel the function of metallo-enzymes to improve knowledge-based drug discovery? *Future Med. Chem.* **2019,** 11, 771-791.

28.   Spinello, A.; Magistrato, A. An omics perspective to the molecular mechanisms of anticancer metallo-drugs in the computational microscope era. *Expert Opin. Drug Discov.* **2017,** 12, 813-825.

29.   Sherman, W.; Day, T.; Jacobson, M. P.; Friesner, R. A.; Farid, R. Novel procedure for modeling ligand/receptor induced fit effects. *J. Med. Chem.* **2006,** 49, 534-53.

30.   Minami, N.; Kijima, S. Reduction of Ortho-Hydroxyaromatic Carboxylic-Acids through Ethoxy-Carbonyl Derivatives with Sodium-Borohydride. *Chem. Pharm. Bull.* **1979,** 27, 816-820.

31.   Gobbi, S.; Hu, Q.; Zimmer, C.; Belluti, F.; Rampa, A.; Hartmann, R. W.; Bisi, A. Drifting of heme-coordinating group in imidazolylmethylxanthones leading to improved selective inhibition of CYP11B1. *Eur. J. Med. Chem.* **2017,** 139, 60-67.

32.   Hevir, N.; Trost, N.; Debeljak, N.; Rizner, T. L. Expression of estrogen and progesterone receptors and estrogen metabolizing enzymes in different breast cancer cell lines. *Chem. Biol. Interact.* **2011,** 191, 206-16.

33.   Vidossich, P.; Magistrato, A. QM/MM molecular dynamics studies of metal binding proteins. *Biomolecules* **2014,** 4, 616-45.

34.   Di Nardo, G.; Breitner, M.; Bandino, A.; Ghosh, D.; Jennings, G. K.; Hackett, J. C.; Gilardi, G. Evidence for an elevated aspartate pK(a) in the active site of human aromatase. *J. Biol. Chem.* **2015,** 290, 1186-96.

35.   Sgrignani, J.; Magistrato, A. First-principles modeling of biological systems and structure-based drug-design. *Curr. Comput. Aided Drug Des.* **2013,** 9, 15-34.

Table of contents